Structural Diversity and Extreme Stability of Unimolecular *Oxytricha nova* Telomeric G-Quadruplex[†]

Ja Yil Lee, Jeongmin Yoon, Hyun Woo Kihm, and D. S. Kim*

Department of Physics and Astronomy, Seoul National University, San 56-1, Shillimdong, Kwanakgu, Seoul, 151-742, South Korea

Received October 7, 2007; Revised Manuscript Received January 4, 2008

ABSTRACT: *Oxytricha nova* telomeric DNA contains guanine-rich short-tandem repeat sequences $(GGGGTTTT)_n$ and terminates as a single strand at the 3′-end. This single-stranded overhang forms a novel DNA structure, namely, G-quadruplex, comprising four quartets. In this study, we investigated the structures and dynamics of unimolecular *Oxytricha nova* (*O. nova*) telomeric G-quadruplexes by performing single molecule fluorescence resonance energy transfer (FRET) spectroscopy and bulk circular dichroism (CD) measurements. We observed that unimolecular *O. nova* G-quadruplexes exhibit structural polymorphism according to monovalent cations. In the presence of Na^+, only antiparallel conformation is detected, which was demonstrated in previous studies; however, in the presence of K^+, they fold into two different conformations, a parallel conformation and an antiparallel one different from that induced by Na^+. Furthermore, these G-quadruplexes show extremely high stability in their dynamics when compared with human G-quadruplexes. While human telomeric G-quadruplexes that possess three quartets display fast dynamic behavior (<100 s) at low K^+ concentrations or high temperatures, *O. nova* G-quadruplexes maintain their conformational state for a long time (>1000 s), even at the lowest K^+ concentration and the highest temperature investigated. This high stability is primarily due to an extra quartet that results in additional cation coordination. In addition to cation coordination, we propose that other factors such as base stacking and the size of the thymine loop may contribute to the stability of *O. nova* G-quadruplexes; this is based on the fact that the *O. nova* G-quadruplexes were observed to be more stable than the human ones in the presence of Li^+, which is known to greatly destabilize G-quadruplexes because of imprecise coordination. This extreme stability of four-quartet G-quadruplexes enables telomere protection even in the absence of protective proteins or in the case of abrupt environmental changes, although only a single G-quadruplex structure can be derived from the short single-stranded overhang.

Telomeres, which are nucleic acid–protein complexes located at the end regions of eukaryotic chromosomes, play an important role in maintaining the stability and integrity of chromosomes (*1–3*). Telomeric DNA comprises short tandem repeats containing many guanines, and the sequence of tandem repeats varies only minutely among organisms (*4, 5*). This guanine-rich single-stranded DNA forms a novel structure *in vitro*, namely, G-quadruplex (*4–7*). Moreover, it has been reported that the G-quadruplex may also exist *in vivo* (*8, 9*). It has received considerable attention because of its structural complexity and biological roles. In particular, the human telomeric G-quadruplex has been extensively studied because it is considered a target for anticancer agents (*10, 11*). Since the parallel structure of the human telomeric G-quadruplex in the presence of K^+ was reported by X-ray crystallography (*12*), its structural polymorphism has received increasing attention, and diverse studies have been performed in this regard (*13, 14*). The coexistence of parallel and antiparallel conformations and their dynamics in a K^+-containing solution was reported by performing single molecule FRET[1] spectroscopy (*15, 16*). More recently, a hybrid-type intramolecular G-quadruplex structure with mixed parallel and antiparallel strands was revealed based on NMR and CD spectra in K^+ solution (*17*).

The telomeric G-quadruplex of *Oxytricha nova* (*O. nova*) has been also extensively investigated to determine various structural and physicochemical characteristics. X-ray crystallography and NMR revealed that bimolecular *O. nova* G-quadruplexes form an antiparallel fold-back structure in the presence of K^+ or Na^+ (*18–20*). The transition between the antiparallel and tetramolecular parallel structure was examined according to cations (*21, 22*). The thermodynamic stability of *O. nova* G-quadruplexes was also investigated and compared by differential scanning calorimetry (*23*). However, most previous studies have focused on the structures and kinetics of bi or tetramolecular quadruplexes. With regard to unimolecular quadruplexes, Wang et al. revealed that the sodium formation of *O. nova* G-quadruplex is an antiparallel fold-back structure (*24*); however, potassium formation of *O. nova* G-quadruplex has not been clearly

[†] This work was supported by MOST, MOCIE, KOSEF, Seoul R&BD, and KRF (Grant Nos. C00012 and C00032).

* Corresponding author. Phone: 82-2-880-8174. E-mail: dsk@phya.snu.ac.kr.

[1] Abbreviations: FRET, fluorescence resonance energy transfer; TMR, tetramethylrhodamine; *O. nova*, *Oxytricha nova*; CD, circular dichroism.

10.1021/bi702013d CCC: $40.75
Published on Web 02/26/2008

demonstrated to date, although potassium ions are more dominant (~140 mM) than sodium ions (~10 mM) in cells (*25*).

In this article, we investigated the structures of the unimolecular *O. nova* G-quadruplex and its dynamics, mainly in the presence of K^+, by using single molecule FRET spectroscopy; this technique makes it possible to eliminate the ensemble-average effect and to observe the conformational dynamics in real time (*26–28*). Consistent with earlier works, single molecule FRET spectroscopy, together with CD spectroscopy, revealed that the unimolecular *O. nova* G-quadruplex folds to the antiparallel conformation in the presence of Na^+. In contrast, we found that in the presence of K^+, this molecule exhibits two different structures, that is, a parallel conformation and an antiparallel one different from that in Na^+. Furthermore, the dynamics of the *O. nova* telomeric G-quadruplexes revealed that these G-quadruplexes are considerably more stable than the human G-quadruplexes. The former maintains either a folded or unfolded conformation for more than 1000 s in the presence of K^+. This extreme stability of *O. nova* G-quadruplexes is due to the presence of four quartets. When compared with the human quadruplexes, an additional cation can be coordinated in the *O. nova* G-quadruplexes because of an additional quartet; this is a major contribution to the extreme stability. In addition, by observing the dynamics in Li^+ solution, we demonstrated that other factors such as base-stacking or the thymine-loop may exert a minor effect on their stability.

MATERIALS AND METHODS

Sample Preparation. Oligomers for bulk FRET and single molecule FRET spectroscopy were purchased from IDT technology. Human and *O. nova* telomeric quadruplex samples were synthesized. Each sample comprised two strands, one corresponding to the G-quadruplex sequences and the other to the stem sequences (Figure 1A) as follows: human G-quadruplex part, 5′-Cy5- GGG TTA GGG TTA GGG TTA GGG AGA GGT AAA AGG ATA ATG GCC ACG GTG CG -Biotin-3′; human stem part, 5′-CGC ACC GTG GCC ATT ATC CTT T*TA CCT CT-3′; *Oxytricha nova* G-quadruplex part, 5′-**Cy5-GGG GTT TTG GGG TTT TGG GGT TTT GGG G**AG AGG TAA AAG GAT AAT GGC CA-**Biotin**-3′; and *Oxytricha nova* stem part, 5′-CCG TGG CCA TTA TCC TT**T*** TAC CTC T-3′. Each 3′-end of the G-quadruplex parts was biotinylated to enable surface attachment. As a donor, tetramethylrhodamine (TMR) was internally labeled by modifying a thymine (**T***) in the stem part, and Cy5 at the 5′-end of the G-quadruplex part served as an acceptor. The G-quadruplex part and stem part were mixed well in a 2:1 ratio and heated to 95 °C. The mixture was then slowly cooled to room temperature.

Bulk Measurements. A spectrofluorometer (F-4500, Hitachi) was used to measure the bulk fluorescence in the presence of various concentrations of potassium at room temperature. Annealed *O. nova* G-quadruplex samples (200 nM) were used. The samples were excited at 532 nm with a bandwidth of 1 nm, and the fluorescence emission was measured from 550 to 750 nm with 1 nm resolution. The fluorescence data was normalized to the TMR emission peak at 580 nm. For CD spectroscopy, oligomers containing only the *O. nova* telomeric sequence, that is, 5′-GGG GTT TTG GGG TTT TGG GGT TTT GGG G-3′, were synthesized (Bioneer, South Korea) in order to exclude the effects of the stem duplex and labeled dyes on the CD spectra. A Jasco J-715 spectropolarimeter was used at room temperature. About 5 μM of samples were prepared in a buffer solution with 10 mM Tris-HCl (pH 7.4) and 200 mM K^+ or Na^+.

Single Molecule Spectroscopy. A microchamber was constructed by bonding a quartz slide (G. Finkenbeiner, USA) and a glass coverslip using double-sided tape. BSA-biotin (A-8549, Sigma) and streptavidin (S-888, Invitrogen) were successively injected. The chamber was cleaned with T50 (10 mM Tris-HCl at pH 7.4 and 50 mM NaCl) between steps. Then 50 ~100 pM of the samples was added, and the chamber was incubated at room temperature for 10 min (*29*). To wash away the nonadherent samples and exclude the effects of Na^+ in the T50 buffer on the G-quadruplexes, the chamber was rinsed with buffer lacking cation (10 mM Tris-HCl at pH 7.4 and 0.4% (w/w) glucose). And the imaging buffer (10 mM Tris-HCl (pH 7.4), 0.4% (w/w) glucose, 1% 2-mercaptoethanol (125472500, Acros), 0.1 mg/mL glucose oxidase (G-2133, Sigma), and 0.02 mg/mL catalase (106810, Roche), which enzymatically reduces the photobleaching of dyes, was injected along with a specific cation concentration (*30*).

Prism-type total internal reflection technique was used for single molecule imaging (*29*). The dyes were excited by using a 532 nm laser (Crystalaser). The fluorescence emitted from each dye was collected by a water-immersion objective lens (60×, 1.2 NA, Olympus) and was then split into donor and acceptor channels via a dichroic mirror (632 DCXR, Chroma Technology). Each channel was imaged on half the area of an intensified CCD (iXon, Andor Technology). The sample temperature was controlled by a homemade apparatus equipped with a thermoelectric device and a water bath (JEIO TECH Co., South Korea). The image was processed with IDL (RSI Inc.), and data analysis was performed by Matlab (The MathWorks Inc.). FRET efficiency was approximated with $I_A/(I_A + I_D)$, where I_A is acceptor intensity, and I_D is donor intensity. FRET histograms were built by averaging FRET efficiency in the first 10 frames for each molecule. The rate constants of the *O. nova* G-quadruplexes in the presence of K^+ were obtained by dividing the number of transitions from one state to the other by the total dwell time in one state. Meanwhile, the rate constants in the presence of Li^+ were obtained by performing dwell time analysis. A histogram of the duration for which molecules remained in a single state was plotted and was then fitted by a single-exponential decay function. The rate constants were calculated by inversing the decay time. The relative population (or duration) of each conformation or species was obtained by dividing its total dwell time by the sum of the dwell time of all of the molecules.

RESULTS

Single Molecule FRET Spectroscopy Unravels the Details of Bulk Results. The normalized ensemble fluorescence spectra of the *O. nova* G-quadruplexes are shown as a function of the potassium concentrations (Figure 1B). The fluorescence of the acceptor (Cy5) increased because of FRET with the addition of K^+ (inset image in Figure 1B). The increase of FRET may occur for two reasons. One reason

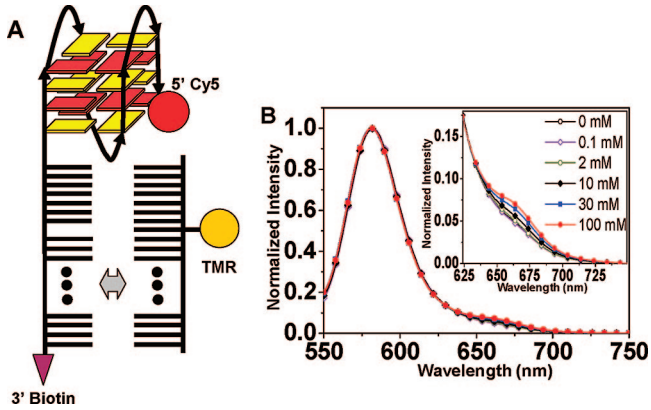

FIGURE 1: Schematic sample configuration and bulk FRET of unimolecular *Oxytricha nova* (*O. nova*) G-quadruplex according to potassium concentration. (A) Schematic diagram of *O. nova* G-quadruplex sample. The sample is composed of two strands, the G-quadruplex part and stem part. TMR (donor) is internally labeled at a thymine in the stem part, and Cy5 (acceptor) is labeled at the 5′-end of the G-quadruplex part. Biotin is modified at the 3′-end of the G-quadruplex part to tether the sample on the quartz slide. (B) Bulk fluorescence spectra as a function of potassium concentrations at room temperature. The samples were excited at 532 nm with 1 nm bandwidth, and the emission was measured from 550 to 750 nm with 1 nm resolution. All spectra were normalized with a TMR (donor) emission peak at 580 nm. Inset: zoomed-in view of Cy5 (acceptor) emission spectra.

may be that the addition of potassium ions induces a gradual structural change in the molecules, reducing the distance between the donor and the acceptor. The other may be that as the K^+ concentration increases, the number of molecules in higher FRET states increases. The details were unraveled by single molecule FRET spectroscopy. Figure 2A shows single molecule FRET histograms obtained for various potassium concentrations. The peak at zero FRET efficiency resulted from molecules whose acceptors were fast photobleached or from those in which only the donor was labeled; thus, this peak could be ignored (*28*). At 10 mM K^+, three distinct FRET peaks other than the zero peak were observed at 0.2 (low), 0.5 (middle), and 0.76 (high), which were obtained by fitting the histogram with multiple Gaussian functions (Figure 2B). In the single molecule FRET histograms, the low peak was highly dominant at low K^+ concentrations, while it disappeared at high K^+ concentrations. In contrast, high and middle FRET peaks were not visible at 0.1 mM K^+ but gradually appeared as the concentration increased. The population histograms represent the conformational states of molecules in equilibrium. This was confirmed by the relative duration of each state (Supporting Information Figure 1), which was accurately consistent with the changes in the population histograms shown in Figure 2A. The single molecule FRET histograms revealed that the increase of FRET occurring in bulk was not derived from a gradual structural change but from the population in higher FRET conformations. Here, it must be noted that the FRET in bulk measurements was considerably lower than that in single molecule spectroscopy because nonannealed donor strands as well as the annealed molecules with the bad acceptor increase only donor fluorescence in bulk.

Unimolecular O. nova Telomeric G-Quadruplexes Fold into Various Conformations Depending on Monovalent Cations. In general, G-quadruplexes are stabilized by the process of cation coordination (*6, 7*). Thus, they are destabilized or unfolded when insufficient cations are present. The addition of cations induces the folding of guanine-rich single strands into G-quadruplexes. As mentioned above, with the addition of potassium ions, the number of molecules in high or middle FRET states increased considerably, while the number in the low FRET state decreased (Figure 2A). Also, when the single-stranded overhang forms a G-quadruplex, it becomes sterically compact, and the distance between the donor and the acceptor is reduced. Therefore, we claim that the low FRET peak represents the unfolded single-stranded overhang, while the high and middle FRET peaks stand for the formation of the folded G-quadruplex. This assignment is compatible with the previous study conducted on human telomeric DNA (*16*). It is possible that Cy5 labeling at the 5′-end and the duplex stem may interfere with the normal formation of G-quadruplexes. However, Ying et al. demonstrated that dye modification and the duplex stem do not affect the formation of G-quadruplexes by using UV melting experiments and CD spectroscopy (*15*).

It is highly interesting that 2-folded structures were observed for the unimolecular *O. nova* G-quadruplex. This indicates that this molecule exhibits structural polymorphism in the presence of K^+. To determine the details of this polymorphism, CD experiments were performed at 200 mM K^+ and Na^+ (Figure 3A). In the presence of Na^+, the CD spectra have a peak at 295 nm and a dip at 265 nm, which are indicative of an antiparallel structure (*23*). However, two distinct peaks appeared at 290 and 260 nm in K^+. In general, the parallel conformation produces a strong positive peak near 260 nm in the CD spectra (*23*). Therefore, we considered the two peaks at 200 mM K^+ in the CD spectra to represent the overlapping of the parallel (peak at 260 nm) and antiparallel (peak at 290 nm) conformations. This suggests that both types of conformations for *O. nova* G-quadruplexes coexist in a K^+-containing solution. The single molecule FRET histograms at 100 mM K^+ and Na^+ are shown in Figure 3B. In the case of Na^+, only a single folded peak appeared at 0.65, which definitely represents an antiparallel conformation based on the above CD results. A previous study revealed that the sodium formation of *O. nova* G-quadruplex is an antiparallel fold-back structure (*23*), and hence, we considered the peak at 0.65 to represent the *antiparallel fold-back conformation*. However, in the presence of K^+, single molecule FRET histogram presented two peaks, like the CD spectra. These peaks shown at two different FRET efficiencies implied that the molecules folded to two different conformations. On the basis of the CD spectra, we considered that the two peaks in the single molecule histogram corresponded to *parallel and antiparallel conformations*. In our sample configuration, the acceptor is located in the bottom quartet in the antiparallel conformation but is near the top quartet in the parallel structure. Sterically, the acceptor is much closer to the donor in the antiparallel conformation than in the parallel one. Therefore, the FRET efficiency of the antiparallel structure is expected to be higher than that of parallel one. This suggests that peaks at the high and middle FRET efficiency correspond to antiparallel and parallel conformations, respectively. In a previous study on human telomeric quadruplexes, 2-folded FRET peaks were observed, and the peaks at high FRET (~0.79) and middle FRET (~0.6) efficiencies were considered to represent the antiparallel and parallel conformations, respec-

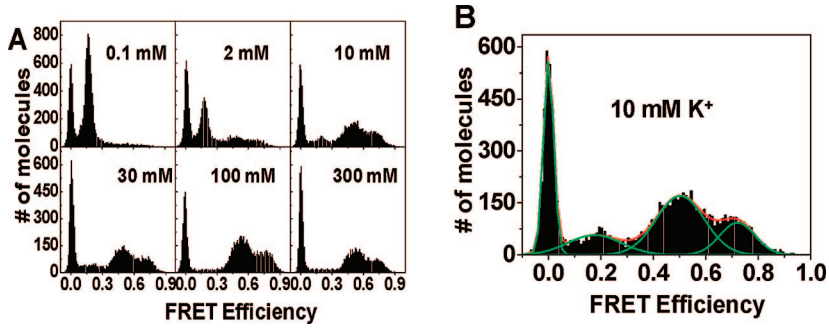

FIGURE 2: Single molecule FRET results of *O. nova* G-quadruplexes. (A) Single molecule FRET histograms of *O. nova* G-quadruplexes for potassium titration. The histograms were built by collecting the FRET values of each molecule, which were averaged for the first 10 frames. (B) Zoomed-in view of the histogram at 10 mM K^+. Three distinct peaks are shown at 0.2, 0.5, and 0.76, except for the peak at zero, which results from imperfect samples.

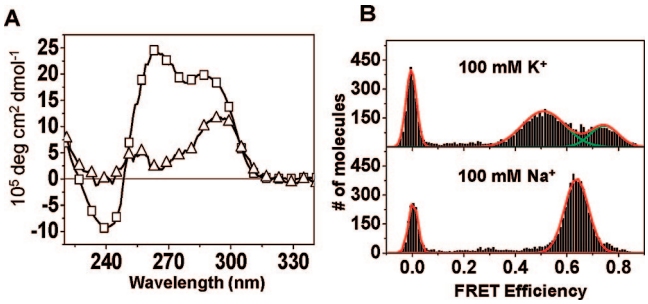

FIGURE 3: Structural polymorphism of unimolecular *O. nova* G-quadruplexes. (A) Circular dichroism spectra of *O. nova* G-quadruplexes at 200 mM K^+ (□) and Na^+ (△). In the presence of K^+, two peaks at 260 and 290 nm are observed, which correspond to parallel and antiparallel conformations, respectively. Meanwhile, one peak and one dip at 295 and 265 nm in Na^+ represent antiparallel structure. (B) Single molecule histograms of *O. nova* G-quadruplexes from single molecule FRET at 100 mM K^+ (top) and Na^+ (bottom). The FRET peaks are fitted by multiple Gaussian functions. Like the CD results, two folded peaks and one folded peak are shown in K^+ and Na^+, respectively.

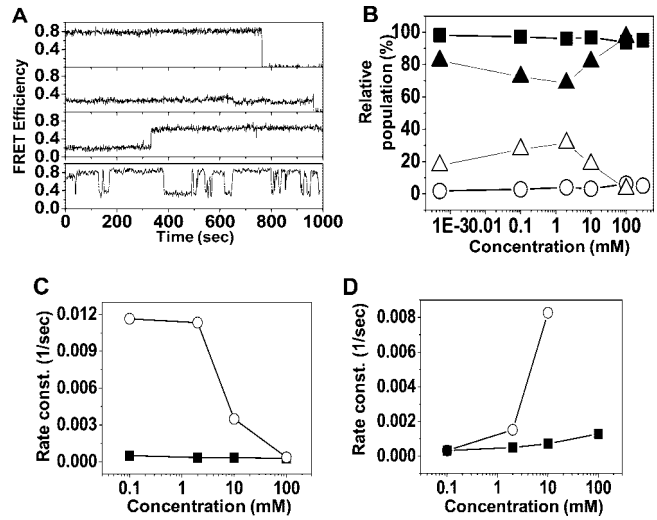

FIGURE 4: Comparison of dynamics between *O. nova* and human G-quadruplexes. (A) Single molecule FRET time traces of *O. nova* (three figures from top) and human G-quadruplex (one figure at bottom) at 2 mM K^+. (B) Relative populations for long- and short-lived species of *O. nova* and human G-quadruplexes; (■), *O. nova* long-lived species; (○), *O. nova* short-lived species; (▲), human long-lived species; and (△), human short-lived species. (C) Unfolding rates and (D) folding rates of *O. nova* (■) and human (○) G-quadruplexes as a function of potassium concentrations. In the case of *O. nova*, the transition to either the folded or the unfolded state is extremely suppressed at all concentrations.

tively (*16*). The configuration of the *O. nova* G-quadruplex in our sample is basically identical to that of the human G-quadruplex, except for the presence of an additional quartet in the former. Because of this additional quartet, the acceptor in the parallel conformation is at a greater distance from the donor; thus, the FRET efficiency in this case is lower than that in humans. In the antiparallel conformation, the position of the acceptor near the bottom quartet is not significantly altered by the additional quartet. Thus, the FRET efficiency in this case is almost equal to that in the human telomeric quadruplex. As expected, the difference in the FRET efficiency of middle FRET peaks is larger (~0.09) than that of high FRET peaks (~0.03). Minor discrepancy in the high FRET peaks results from a quartet twist due to glycosidic torsion (*6, 7*). This highly supports our interpretation of the high and middle FRET peaks obtained for the *O. nova* G-quadruplexes. It is noteworthy that the FRET efficiency of the antiparallel peak in the presence of K^+ differs from that of the peak in the presence of Na^+. This implies that the antiparallel conformations differ in the presence of K^+ and Na^+; however, our results are insufficient to describe the conformations in greater detail.

O. nova G-Quadruplexes Exhibit Extreme Stability as Compared to Human G-Quadruplexes. Most *O. nova* G-quadruplexes fold and are stabilized at high potassium concentrations (Figure 2A and Supporting Information Figure 1A). To investigate the intrinsic behavior of these quadruplexes, we observed the dynamics of the molecules at a low potassium concentration. Single molecule time traces of the *O. nova* and human telomeric G-quadruplexes at 2 mM K^+ are shown (Figure 4A). The *O. nova* G-quadruplexes maintained their conformational state (folded or unfolded) for a long time (>700 s) and rarely underwent transition between the folded and unfolded states. In contrast, human G-quadruplexes frequently underwent transition between the folded and unfolded states within the same time window. Heterogeneity in dynamics has been reported for human G-quadruplexes (*16*). Molecules occasionally remain in a particular conformational state for a long time (>100 s, *long-lived species*) and occasionally fluctuates rapidly between the folded and unfolded conformations (<100 s, *short-lived species*). Considering the same criteria, *O. nova* G-quadruplexes did not show heterogeneous dynamics at any potassium concentrations. Figure 4B shows the relative population of long-lived and short-lived species as a function of K^+

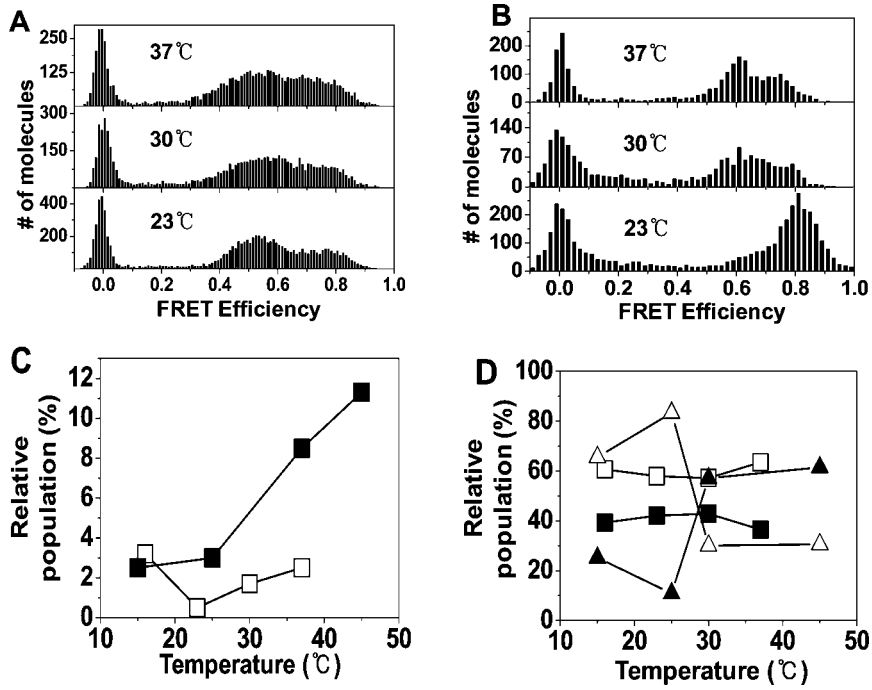

FIGURE 5: Temperature dependence of the dynamics of *O. nova* and human G-quadruplexes at 100 mM K^+. Single molecule histograms of (A) *O. nova* and (B) human G-quadruplexes according to temperature. (C) Relative population of short-lived species in *O. nova* (□) and human (■) G-quadruplexes. (D) Relative population of parallel conformation of *O. nova* (■) and human (▲) G-quadruplexes, and antiparallel conformation of *O. nova* (□) and human (△) G-quadruplexes. The relative population of each conformation or species was obtained by dividing its own total dwell time by the total sum of the dwell time of all molecules.

concentrations. Each of the species includes both the folded and unfolded states. In the human G-quadruplexes, the short-lived species are maximally populated at 2−10 mM K^+ and play an intermediate role between the long-lived unfolded state at low K^+ concentrations and the long-lived folded state at high K^+ concentrations. In contrast, the percentage of short-lived species was less than 4% at all concentrations in the case of *O. nova*. Thus, the short-lived species were completely suppressed, regardless of the potassium concentration.

To quantitatively analyze the dynamics of the *O. nova* and human G-quadruplexes, the rates of transition between the folded and unfolded states were determined as a function of the potassium concentrations (Figure 4C and D). The transition rates of the human G-quadruplexes are highly sensitive to the potassium concentration. The unfolding rates decrease (or the folding rates increase) sharply with the addition of potassium ions. At low K^+ concentrations, the molecules unfold immediately after they have folded into G-quadruplexes, while at high K^+ concentrations, they refold immediately after they have been unfolded. This behavior is mainly due to the short-lived species that determine the overall dynamics in human G-quadruplexes (*16*). The transition rates of *O. nova* G-quadruplexes are almost constant and much lower ($\sim 10^{-4}$ s^{-1}) than those of human G-quadruplexes (*16*). This indicates that folding (or unfolding) is a more laborious process in *O. nova* G-quadruplexes than in human G-quadruplexes; hence, the former are more energetically stable than the latter.

Thermal energy destabilizes G-quadruplexes (*31*). To investigate their stability with regard to temperature, we heated both human and *O. nova* G-quadruplexes at 100 mM K^+. In both cases, a large number of molecules still remained in the folded states despite the increase in temperature (Figure 5A and B). However, the two types of quadruplexes exhibited a discrepancy in the underlying dynamics. We examined the relative population of short-lived species in the human and *O. nova* G-quadruplexes (Figure 5C). The short-lived species in the *O. nova* G-quadruplexes remained suppressed, whereas those in the human G-quadruplexes got populated as the temperature increased. In human quadruplexes, the short-lived species mediated the conformational transition from the antiparallel to the parallel state (Figure 5D). In contrast, the number of molecules in the parallel and antiparallel conformations does not change in the *O. nova* G-quadruplexes because of the suppression of short-lived species. Consequently, *O. nova* G-quadruplexes exhibit greater thermal stability than human quadruplexes.

O. nova G-Quadruplexes Are Destabilized by Weakly Coordinated Li^+. It is well-known that lithium ions bind weakly to G-quadruplexes and cannot stabilize them since their ionic size is too small to enable efficient coordination in the cavity between G-tetrads (*6, 7*). Therefore, we investigated the conformational dynamics of G-quadruplexes in situations where cation coordination does not strongly affect their stability. Destabilization was observed in the single molecule FRET time traces (Figure 6A and Supporting Information Figure 2), where the molecules did not retain their folded state (high FRET) for a long time even at high Li^+ concentrations. FRET histograms obtained for the *O. nova* and human G-quadruplexes at various Li^+ concentrations are shown (Figure 6B and C). At a low Li^+ concentration (10 mM), only one peak other than the peak at zero FRET appeared at 0.2 and 0.25 for the *O. nova* and human G-quadruplexes, respectively. During potassium titration, this peak was already considered to arise from the unfolded single-stranded overhang. The difference in FRET efficiency among unfolded conformations resulted from the length of

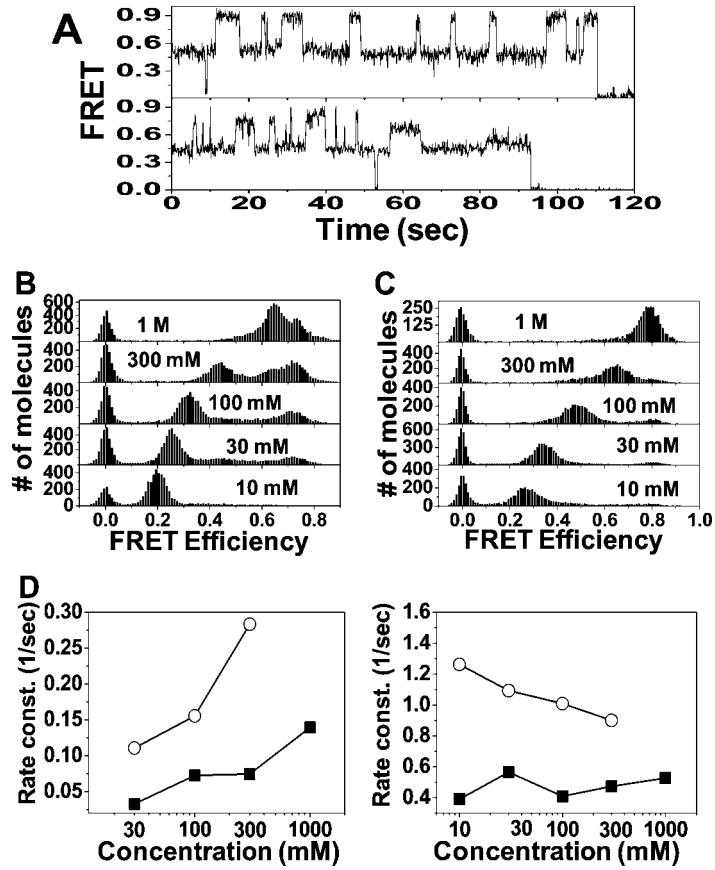

FIGURE 6: Destabilization of *O. nova* and human G-quadruplexes at room temperature in the presence of Li^+. (A) Single molecule FRET time traces of *O. nova* (top) and human (bottom) G-quadruplex at 300 mM Li^+. Even at the high concentration, only short-lived species are observed. Single molecule FRET histograms for (B) *O. nova* and for (C) human G-quadruplexes. For both cases, the unfolded peak still survives and moves to higher FRET as the concentration increases. Transition rates as a function of Li^+ concentrations: (D) folding rates of *O. nova* (■) and human (○) G-quadruplexes, and (E) unfolding rates of *O. nova* (■) and human (○) G-quadruplexes. The transition rates of human G-quadruplexes at 1 M could not be obtained because the unfolded and folded FRET states were indistinguishable.

the single-stranded overhang. It is important to note that almost all molecules were in the unfolded state at this Li^+ concentration, whereas many of them were folded at the same concentration of K^+ (Figure 2A). This confirms that G-quadruplexes are destabilized by Li^+. Interestingly, the unfolded peak gradually shifted toward higher FRET efficiency as the Li^+ concentration was increased. This phenomenon was clearly observed in the single molecule time traces (Supporting Information Figure 2). This shift arises from the charge screening effect, wherein cations bind to the negatively charged DNA backbone, thus increasing the flexibility of the single-stranded overhang (*32*). In both types of G-quadruplexes, the unfolded peak survived even at high Li^+ concentrations because Li^+ cannot stabilize these G-quadruplexes as strongly as K^+ does. In the *O. nova* G-quadruplexes, the second peak arose at 0.75 at 30 mM Li^+, and another peak at 0.64 appeared at 300 mM Li^+. In contrast, only a single folded peak was obtained for human G-quadruplexes at 0.79. Notably, the concentration at which the folded peak appeared was higher for human G-quadruplexes (~100 mM) than for the *O. nova* ones (~30 mM). Through dwell time analysis for the short-lived species, the folding and unfolding rates were obtained as a function of the concentrations (Figure 6D and E). The rate constants at 1 M Li^+ could not be determined in the human G-quadruplexes because the unfolded states could not be distinguished from the folded states. In both types of quadruplexes, the unfolding rates in the presence of Li^+ are approximately 10^3-fold higher than those in the presence of K^+, indicating that the coordination of Li^+ has only a small effect on the stabilization of G-quadruplexes. The unfolding and folding rates of the *O. nova* G-quadruplexes were 2- or 3-fold lower than those of the human G-quadruplexes, regardless of Li^+ concentrations (Figure 6D and E). This demonstrates that *O. nova* G-quadruplexes are more stable than human ones, even when the cation coordination is not dominant.

DISCUSSION

Structural polymorphism is one of the important issues with regard to G-quadruplexes because their structure may significantly affect their biological functions *in vivo* (*10, 11, 33*). We found that the unimolecular *O. nova* G-quadruplexes form two types of folded structures, that is, parallel and antiparallel conformations, in the presence of K^+. In the presence of Na^+, however, they present only a single structure, that is, an antiparallel conformation that differs from that in the presence of K^+. For the unimolecular human telomeric G-quadruplex, different types of antiparallel conformations were proposed (*14*). Similarly, the unimolecular *O. nova* G-quadruplexes can form different types of antiparallel conformations, although we were unable to demonstrate the details of these structures. Interestingly, in addition to the antiparallel conformation, the unimolecular *O. nova*

G-quadruplex exhibits a parallel conformation in K^+. In bulk solutions, it is possible that a four-stranded parallel structure may develop. However, Qi et al. reported that the four-stranded parallel conformation of unimolecular quadruplexes is not dominant in K^+ solution by native gel experiments (*13*). Although the possibility of four-stranded parallel quadruplexes occurring in bulk solution cannot be completely excluded, we can guarantee that, in single molecule experiments, unimolecular *O. nova* G-quadruplexes only form the intrastrand parallel structure becaue of the absence of interaction among individual molecules. With regard to this intrastrand parallel conformation, two possibilities can be considered. The first possibility is a propeller-like parallel structure similar to the potassium formation of human telomeric G-quadruplex that was reported by Parkinson et al. via X-ray crystallography (*12*). The second possibility is a hybrid structure comprising a combination of parallel and antiparallel strands (*17*). The CD spectra of this hybrid structure exhibit double peaks at 268 and 290 nm, similar to our results. The configuration of the donor and acceptor in this hybrid structure is identical to that in the propeller-like parallel conformation, and hence, the hybrid structure could exhibit a peak at 0.5. This structural diversity of unimolecular *O. nova* G-quadruplexes *in vitro* according to monovalent cations implies that the folded conformation is altered depending on the surrounding conditions, and hence, the interaction of these quadruplexes with external biomolecules is also expected to change *in vivo*.

In the presence of K^+, the dynamics of the *O. nova* G-quadruplexes differs remarkably from that of the human quadruplexes. On the basis of our quantitative analysis, the folding and unfolding rates of the *O. nova* G-quadruplexes are by far lower than those of the human ones. These results imply that the energy barrier between the folded and unfolded conformations is considerably higher in the case of *O. nova* quadruplexes when compared with human G-quadruplexes. Previous X-ray crystallographic experiments have revealed that *O. nova* G-quadruplexes possess three cation binding sites (*18*), that is, one site more than human G-quadruplexes possess (*12*). This additional coordination increases the energy barrier between the folded and unfolded states. Consequently, the folded (unfolded) states last for a long time at low (high) K^+ concentrations despite the small number of molecules in these states. It is noteworthy that the short-lived species in *O. nova* G-quadruplexes are highly suppressed in the presence of K^+. This induces the all-or-nothing behavior of *O. nova* G-quadruplexes. In other words, no intermediate energy states between the folded and unfolded conformations exist in these G-quadruplexes. On the basis of the dynamics observed in the presence of Li^+, the origin of short-lived species appears to be weak or imperfect cation coordination. Thus, the single-stranded overhang of the *O. nova* telomeric sequence only folds into the G-quadruplex once it has taken up enough cations to stabilize the four quartets by perfect coordination, and it is completely stabilized. However, the folded molecules unfold and become stable by discarding all of the cations that they had taken up.

During Li^+ titration, *O. nova* G-quadruplexes show greater stability than the human ones. This higher stability is reflected well in the dynamics of the quadruplexes in that the overall transition rates of the former are 2- or 3-fold lower than those of the latter. Li^+ is known to destabilize G-quadruplexes because of highly weak and imprecise coordination (*6, 7*). Even when the coordination effect is greatly diminished by Li^+, *O. nova* G-quadruplexes are more stable than human ones. This suggests that factors other than cation coordination may contribute to the stability of the four-quartet G-quadruplexes, although the effects of the increased number of coordinated lithium ions on their stability cannot be completely ignored. As mentioned above, the *O. nova* G-quadruplex possesses one quartet more than the human one. Thus, four additional double hydrogen bonds are formed between guanines in this extra quartet. In addition, base stacking probably contributes to the higher stability of the four-quartet quadruplexes. Base stacking is one of the crucial stabilizing factors for single- or double-stranded DNA and is made up of the London dispersion force and hydrophobic interaction (*34*). Especially, G-quadruplex structure involves the stacking of four bases, and hence, the stacking effect is stronger than that of B-DNA. Another possible contributing factor is that the side loop of the *O. nova* G-quadruplex possesses one thymine residue more than that of the human G-quadruplex. G-quadruplexes with four-thymine loops are reported to be energetically more stable than those with three-thymine loops (*35*).

The basic role of telomeres in eukaryotic cells is to protect the degradation of chromosomes. In humans, the end of the telomeres consists of a single strand of about 1−2 kb and forms novel structures, namely, D-loop and t-loop (*36*), and furthermore is protected by proteins such as POT1 that bind to the single strand. The G-quadruplex that is occasionally formed in telomeres is also considered as one of the protective mechanisms against external intrusions (*10*). Moreover, the possibility of multiple G-quadruplexes has been suggested for higher-order compaction in human telomeres (*17, 33*). In contrast to the human telomeres, the end of *O. nova* telomeres comprises an extremely short single strand (about 12 nt) that can only form a single G-quadruplex. Although TEBPα and TEBPβ may function in shielding the telomere (*37–39*), the telomere should be protected from external disturbances and should be maintained even in the absence of protecting proteins or in the cases of the abrupt changes in the environmental conditions. This may explain why *O. nova* G-quadruplexes comprise four quartets and are extremely stable.

ACKNOWLEDGMENT

We appreciate the advice provided by Professor S. Hohng of Department of Physics and Astronomy, Seoul National University. We thank Professor T. Ha of Howard Hughes Medical Institute and Department of Physics, University of Illinois for helpful discussions and support. We also thank Professor S. Hong of Department of Physics and Astronomy, Seoul National University for the generous provision of utilities.

SUPPORTING INFORMATION AVAILABLE

Relative durations of each conformational state of *O. nova* G-quadruplexes and single molecule FRET time traces of *O. nova* G-quadruplexes as a function of Li^+. This material is available free of charge via the Internet at http://pubs.acs.org.

REFERENCES

1. Blackburn, E. H. (1991) Structure and function of telomeres. *Nature 350*, 569–573.
2. Zakian, V. A. (1995) Telomeres: beginning to understand the end. *Science 270*, 1601–1607.
3. Greider, C. W. (1996) Telomere length regulation. *Annu. Rev. Biochem. 65*, 337–365.
4. Neidle, S, and Parkinson, G. N. (2003) The structure of telomeric DNA. *Curr. Opin. Struct. Biol. 13*, 275–283.
5. Anzai, T., Takahashi, H., and Fujiwara, H. (2001) Sequence-specific recognition and cleavage of telomeric repeat $(TTAGG)_n$ by endonuclease of non-long terminal repeat retrotransposon TRAS1. *Mol. Cell. Biol. 21*, 100–108.
6. Davis, J. T. (2004) G-quartets 40 years later: from 5′-GMP to molecular biology and supramolecular chemistry. *Angew. Chem., Int. Ed. 43*, 668–698.
7. Simonsson, T. (2001) G-quadruplex DNA structures-variation on a theme. *Biol. Chem. 382*, 621–628.
8. Schaffitzel, C., Berger, I., Postberg, J., Hanes, J., Lipps, H. J., and Pluckthun, A. (2001) In vitro generated antibodies specific for telomeric guanine-quadruplex DNA react with *Stylonychia lemnae* macronuclei. *Proc. Natl. Acad. Sci. U.S.A. 98*, 8572–8577.
9. Duquette, M. L., Handa, P., Vincent, J. A., Taylor, A. F., and Maizels, N. (2004) Intracellular transcription of G-rich DNAs induces formation of G-loops, novel structures containing G4 DNA. *Gene Dev. 18*, 1618–1629.
10. Zahler, A. M., Williamson, J. R., Cech, T. R., and Prescott, D. M. (1991) Inhibition of telomerase by G-quartet DNA structures. *Nature 350*, 718–720.
11. Neidle, S., and Parkinson, G. (2002) Telomere maintenance as a target for anticancer drug discovery. *Nat. Rev. Drug Discovery 1*, 383–393.
12. Parkinson, G. M., Lee, M. P. H., and Neidle, S. (2002) Crystal structure of parallel quadruplexes from human telomeric DNA. *Nature 417*, 876–880.
13. Qi, J., and Shafer, R. H. (2005) Covalent ligation studies on the human telomere quadruplex. *Nucleic Acids Res. 33*, 3185–3192.
14. He, Y., Neumann, R. D., and Panyutin, I. G. (2004) Intramolecular quadruplex conformation of human telomeric DNA assessed with ^{125}I-radioprobing. *Nucleic Acids Res. 32*, 5359–5367.
15. Ying, L., Green, J. J., Klenerman, D., and Balasubramanian, S. (2003) Studies on the structure and dynamics of the human telomeric G quadruplex by single-molecule fluorescence resonance energy transfer. *Proc. Natl. Acad. Sci. U.S.A. 100*, 14629–14634.
16. Lee, J. Y., Okumus, B., Kim, D. S., and Ha, T. (2005) Extreme conformational diversity in human telomeric DNA. *Proc. Natl. Acad. Sci. U.S.A. 102*, 18938–18943.
17. Ambrus, A., Chen, D., Dai, J, Bialis, T., Jones, R. A., and Yang, D. 2006) Human telomeric sequence forms a hybrid-type intramolecular G-quadruplex structure with mixed parallel/antiparallel strands in potassium solution *Nucleic Acid Res. 34*, 2723–2735.
18. Haider, S., Parkinson, G. N., and Neidle, S. (2002) Crystal structures of the potassium form of an *Oxytricha nova* G-quadruplex. *J. Mol. Biol. 320*, 189–200.
19. Schultze, P., Smith, F. W., and Feigon, J. (1994) Refined solution structure of the dimeric quadruplex formed from the *Oxytricha* telomeric oligonucleotide d(GGGGTTTTGGGG). *Structure 2*, 221–233.
20. Smith, F. W., and Feigon, J. (1992) Quadruplex structure of *Oxytricha* telomeric DNA oligonucleotides. *Nature 356*, 164–167.
21. Miura, T., and Benevides, J. M., Jr. (1995) A phase diagram for sodium and potassium ion control of polymorphism in telomeric DNA. *J. Mol. Biol. 248*, 233–238.
22. Miyoshi, D., Nakao, A., and Sugimoto, N. (2003) Structural transition from antiparallel to parallel G-quadruplex of $d(G_4T_4G_4)$ induced by Ca^{2+}. *Nucleic Acids Res. 31*, 1156–1163.
23. Petraccone, L., Erra, E., Esposito, V., Randazzo, A., Mayol, L., Nasti, L., Barone, G., and Giancola, C. (2004) Stability and structure of telomeric DNA sequences forming quadruplexes containing four G-tetrads with different topological arrangements. *Biochemistry 43*, 4877–4884.
24. Wang, Y., and Patel, D. J. (1995) Solution structure of the *Oxytricha* telomeric repeat $d[G_4(T_4G_4)_3]$ G-tetraplex. *J. Mol. Biol. 251*, 76–94.
25. Albert, B., Bray, D., Hopkin, K., Johnson, A., Lewis, J., Raff, M., Robert, K., and Walter, P. (2004) *Essential Cell Biology*, 2nd ed., p 390, Garland Science, NewYork.
26. Rigler, R., Orrit, M., and Basche, T. (2001) *Single Molecule Spectroscopy: Nobel Conference Lectures* (Moerner, W. E., Ed.) 1st ed., pp 32–34, Springer-Verlag, Berlin, Heidelberg, and New York.
27. Zander, C., Enderlein, J., and Keller, R. A. (2002) *Single Molecule Detection in Solution - Methods and Applications* (Zander, C., Ed.) 1st ed., pp 247–269, *WILEY-VCH*, Berlin.
28. Weiss, S. (1999) Fluorescence spectroscopy of single biomolecules. *Science 283*, 1676–1683.
29. Hohng, S., Wilson, T. J., Tan, E., Clegg, R. M., Lilley, D. M. J., and Ha, T. (2004) Conformational flexibility of four-way junctions in RNA. *J. Mol. Biol. 336*, 69–79.
30. Yildiz, A., Forkey, J. N., McKinney, S. A., Ha, T., Golman, Y. E., and Selvin, P. R. (2003) Myosin V walks hand-over-hand: single fluorophore imaging with 1.5-nm location. *Science 300*, 2061–2065.
31. Mergny, J. L., Phan, A. T., and Lacroix, L. (1998) Following G-quartet formation by UV-spectroscopy. *FEBS Lett. 435*, 74–78.
32. Murphy, M. C., Rasnik, I., Cheng, W., Lohman, T. M., and Ha, T. (2004) Probing single-stranded DNA conformational flexibility using fluorescence spectroscopy. *Biophys. J. 86*, 2530–2537.
33. Patel, D. J. (2002) A molecular propeller. *Nature 417*, 807–808.
34. Müller-Dethlefs, K., and Hobza, P. (2000) Noncovalent interactions: a challenge for experiment and theory. *Chem. Rev. 100*, 143∼167.
35. Balagurumoorthy, P., Brahmachari, S. K., Mohanty, D., Bansal, M., and Sasisekharan, V. (1992) Hairpin and parallel quartet structures for telomeric sequences. *Nucleic Acids Res. 20*, 4061–4067.
36. Greider, C. W. (1999) Telomere do D-loop-t-loop. *Cell 97*, 419–422.
37. Paeschke, K., Simonsson, T., Postberg, J., Rhodes, D., and Lipps, H. J. (2005) Telomere end-binding proteins control the formation of G-quadruplex DNA structure in vivo. *Nat. Struct. Mol. Biol. 12*, 847–854.
38. Lange, T. D. (2001) Telomere capping—one strand fits all. *Science 292*, 1075–1076.
39. Horvath, M. P., Schweiker, V. L., Bevilacqua, J. M., Ruggles, J. A., and Schultz, S. C. (1998) Crystal structure of the *Oxytricha nova* telomere end binding protein complexed with single strand DNA. *Cell 95*, 963–974.

BI702013D